Available online at www.sciencedirect.com
ScienceDirect
Trans. Nonferrous Met. Soc. China 26(2016) 2355−2362
Transactions of Nonferrous Metals Society of China
www.tnmsc.cn

Effect of pre-annealing on microstructure and compactibility of gas-atomized Al−Si alloy powders

Zhi-yong CAI[1,2], Chun ZHANG[1,2], Ri-chu WANG[2], Chao-qun PENG[2], Ke QIU[2], Nai-guang WANG[2]

1. School of Materials Science and Engineering, Jiangxi University of Science and Technology, Ganzhou 341000, China;
2. School of Materials Science and Engineering, Central South University, Changsha 410083, China

Received 11 September 2015; accepted 6 May 2016

Abstract: Effect of pre-annealing treatment temperature on compactibility of gas-atomized Al−27%Si alloy powders was investigated. Microstructure and hardness of the annealed powders were characterized. Pre-annealing results in decreasing Al matrix hardness, dissolving of needle-like eutectic Si phase, precipitation and growth of supersaturated Si atoms, and spheroidisation of primary Si phase. Compactibility of the alloy powders is gradually improved with increasing the annealing temperature to 400 °C. However, it decreases when the temperature is above 400 °C owing to the existence of Si−Si phase clusters and the densely distributed Si particles. A maximum relative density of 96.1% is obtained after annealing at 400 °C for 4 h. In addition, the deviation of compactibility among the pre-annealed powders reaches a maximum at a pressure of 175 MPa. Therefore, a proper pre-annealing treatment can significantly enhance the cold compactibility of gas-atomized Al−Si alloy powders.
Key words: Al−Si alloy; compactibility; rapid solidification; annealing; microstructure

1 Introduction

Rapidly solidified materials have superior mechanical properties, such as high strength, modulus, wear resistance, and elevated temperature strength [1−3]. This comes from the reduction of segregation, refinement of secondary phases or intermetallic compounds and suppression or elimination of coarse primary phases, which results from high solidification rate. In this sort of application, gas-atomization is a well-established technology for fabricating pure or pre-alloyed powder [4,5]. It is generally known that the powder compactibility plays an important role in the economical production of powder metallurgy (PM) route. Therefore, it is important to understand the powder compactibility thoroughly in terms of densification and microstructure variations to control the consolidation process, and then the characteristics of bulk material [6−8].

As a precursor process to sintering or other hot working, many studies have been carried out on the compactibility of metal, ceramic, and composite powder [9−11]. Previous studies indicated that reinforcement characteristics, such as size, shape, and distribution, have a great effect on the densification behavior [6,12,13]. DELIE and BOUVAR [6] suggested that irregular reinforcements hinder the densification behavior, especially when the volume fraction of reinforcement is high or when the reinforcements have high aspect ratio. Their numerical simulation results indicated that the matrix should be more deformed to surround the reinforcements with high specific area. The compactibility is also reduced with decreasing the size of reinforcement or increasing its volume fraction [14−16]. Mechanical milling, towards a homogeneous distribution of reinforcement, not only changes the powder microstructure, mechanical properties, and morphology, but also influences the compactibility [17−19]. Increasing the milling time results in enhancing the matrix hardness and the formation of spherical powder, which reduces the deformation capacity [18].

In terms of microstructure and performance, hypereutectic Al−Si alloy is generally regarded as an in-situ natural Al matrix composite, in which Si phases act as reinforcement [20,21]. According to the classical

Foundation item: Project (JPPT-125-GJGG-14-016) supported by Military Supporting Projects of National Defense Science and Technology Industry Committee, China
Corresponding author: Chun ZHANG; Tel: +86-797-8312555; E-mail: czhangmse@163.com
DOI: 10.1016/S1003-6326(16)64357-1

LSW theory [22,23], the grains are coarsened as a function of temperature and holding time. What's more, the Si phase characteristics in rapidly solidified Al−Si alloys are highly sensitive to the annealing temperature [24,25]. Therefore, the evolution of Si phases, i.e., size, shape, and morphology, and the mechanical properties of Al matrix will significantly affect the compactibility of rapidly solidified hypereutectic Al−Si alloy powder. According to the open literatures available, no study has been reported on the effect of pre-annealing treatment on the compaction behavior of rapidly solidified powder.

In the present work, the compactibility of gas-atomized hypereutectic Al−Si alloy powder was evaluated as a function of pre-annealing temperature. The effect of pre-annealing temperature on the evolution of α(Al) matrix microhardness and the characteristic of Si phases, including primary and eutectic Si phases were investigated. The morphology of the Si phases was observed from powder particle cross-sectional and surface microstructures and the Si phases extracted from the Al matrix by deep etching. Finally, the microstructural features and matrix hardness effects on powder compactibility were discussed based on density versus applied pressure curves obtained by cold rigid compaction.

2 Experimental

Hypereutectic Al−27%Si (all compositions are in mass fraction) alloy powders were employed in the present work. The master alloy prepared by induction melting process was melted at 950 °C. High purity Al (99.995%) and monocrystalline silicon (99.999%) were utilized as raw materials. The molten metal was poured into a tundish and then bottom poured through a graphite melt delivery nozzle of 2.5 mm into an annular N_2 gas atomizer operating at a pressure of 0.9 MPa. The as-atomized alloy powders were mechanically sieved to exclude particles larger than 200 μm.

The powders were pre-annealed at various temperatures (100 to 450 °C) for 4 h under the atmosphere of H_2. Compactions of the as-atomized and pre-annealed powder were conducted at room temperature in a cylindrical die with an inner diameter of 20 mm. In each case, the pressure was slowly increased to the target value and held for 30 s before ejection of the die. The initial aspect ratio of L_0/d (height/diameter) was lower than 0.5 to ensure more homogeneous pressure distribution into the cylindrical sample. The die was not lubricated and no lubricant was mixed into the powder.

Size characteristics of the as-atomized powders were analyzed using a laser particle size analyzer. Specimens for microstructural observation were prepared and etched with Keller's reagent (1%HF−1.5%HCl−2.5%HNO_3−95%H_2O, volume fraction). To reveal the morphology of primary and eutectic Si phases in more detail, the as-atomized and annealed powders were deep-etched with 10% HCl dilute reagent at 60 °C, respectively. The morphology and microstructure of powders and the Si phase morphology were characterized by using a scanning electron microscope (SEM, FEI QUANTA−200). The Vickers microhardness was measured by applying a load of 10 g for 30 s. At least 20 measurements were made randomly on the polished particle cross-sections. The size characteristics of the Si phase were measured using an image analysis software. The relative densities of compacts were measured by the Archimedes immersion method and volumetric method, respectively. The Archimedes method indicates that the apparent mass of an object immersed in water decreases by an amount equal to the volume of the liquid that it displaces. While, the volumetric method is according to the volume and mass of an object. It was noted that the Archimedes results may be not accurate for compacts with high porosity, thus the volumetric results were used when the disagreement between values from Archimedes and volume method was above 2.0%.

3 Results and discussion

3.1 Powder morphology and size distribution

It is widely realized that the compaction behavior and consolidation process of PM parts are strongly affected by the powder characteristics such as morphological features, microstructure, mechanical properties, size, and size distribution [16]. Figure 1 presents the morphologies of the gas-atomized Al−Si alloy powders. From the images, the powder particles have various shapes, such as teardrop, ellipsoid or near spherical (Fig. 1(a)). The surface of the particles is quite rough, with many satellite particles, flasher or holes (Fig. 1(b)). With decreasing the particle size, the particles with near spherical shape become dominant and the surfaces become smoother. Size distribution characteristics of the powders are presented in Table 1.

Table 1 Size distribution characteristic of hypereutectic Al−Si alloy powders (D_n is the particle diameter (μm) at n percent of cumulative curve, D_v is the mean particle diameter from volume, and D_a is the mean particle diameter from area)

Parameter	Particle size/μm
D_{10}	16.0
D_{50}	50.5
D_{90}	110.5
D_v	57.7
D_a	28.1

3.2 Microstructure and hardness

Figure 2 shows the cross-sectional microstructures of the Al−Si alloy powders with a diameter of about 30 μm as a function of the pre-annealing temperature. Irregular primary Si phase with sharp corners and needle-like eutectic Si phase with network structure distribute in Al matrix at the as-atomized state (Fig. 2(a)). After annealing at 300 °C, the eutectic Si phase partially dissolves into the Al matrix as the aspect ratio (the ratio of needle length to width) decreases. While, no obvious change in the size and shape of the primary Si phase appears (Fig. 2(b)). After annealing at

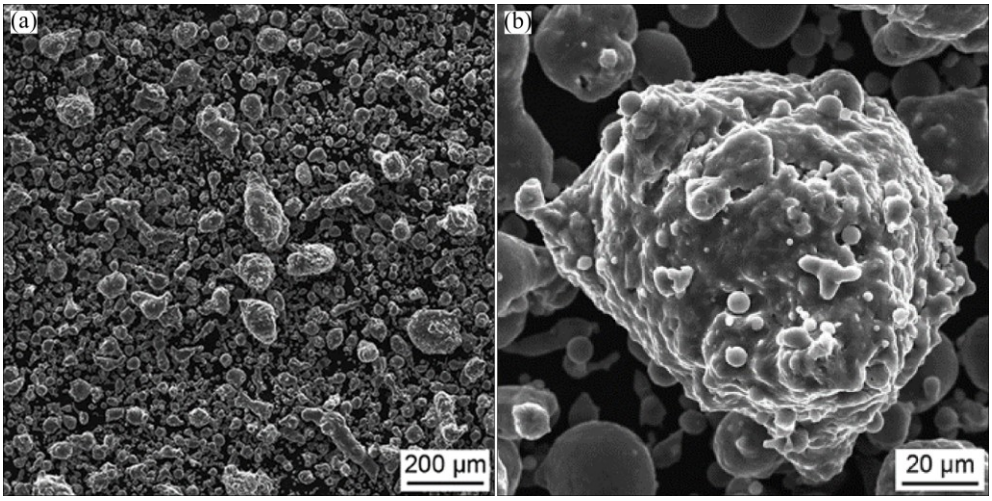

Fig. 1 Morphological features of Al−Si alloy powders with various shapes depending on particle size (a) and quite rough powder surface (b)

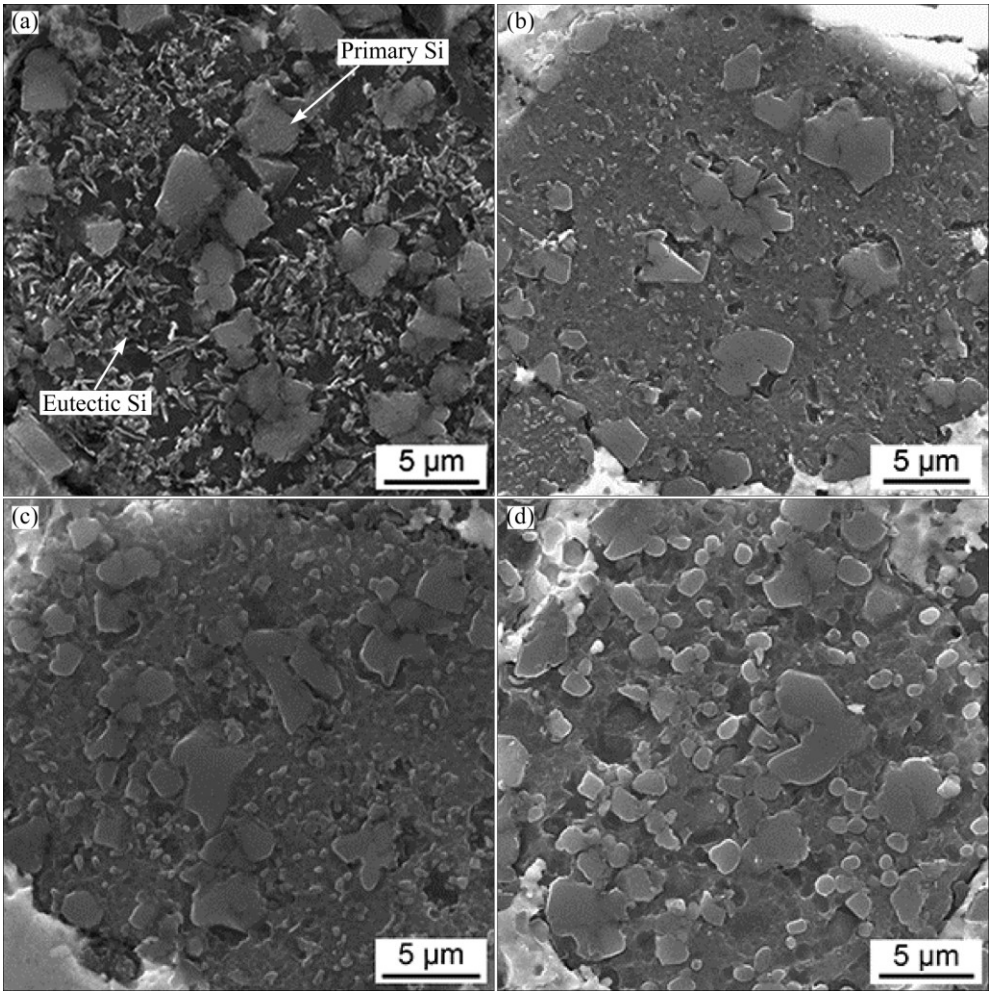

Fig. 2 Microstructures of Al−Si alloy powders as-atomized (a) and pre-annealed at 300 °C (b), 400 °C (c) and 450 °C (d)

400 °C, the Si crystals precipitate from the supersaturated Al matrix and then grow to have an approximately spherical shape (Fig. 2(c)). Thus, the rapidly solidified structure finally decomposes into two equilibrium phases of α(Al) and Si phase by annealing. In the powders pre-annealed at 450 °C, the newly formed Si phase and the primary Si phase quickly grow to have a mean diameter of 1.76 μm and 4.56 μm, respectively (Fig. 2(d)). Another important phenomenon is also noticed that the volume fraction of Si phase seems to gradually increase with increasing the temperature owing to the precipitation and growth of supersaturated Si.

As reinforcement, the characteristic of Si phases, including primary and eutectic phases, can greatly influence the compaction behavior of hypereutectic Al−Si alloy powders. In order to investigate the morphologies of the Si phases in more detail, Si phases were extracted from the Al matrix through deep-etching and the results are shown in Fig. 3. From Fig. 3, it is observed that the pre-annealing temperature has a significant effect on the morphologies of primary and eutectic Si phases. The primary Si phase exhibits a variety of morphologies such as polygonal, star-like, and other irregular shapes in the as-atomized state (Fig. 3(a)). However, the spheroidizing of primary Si phase is observed as the sharp corners become smoother after pre-annealing, as shown in Figs. 3(b) to (d). Furthermore, clustering of the primary Si phase is observed after pre-annealing at 450 °C, where the clustered Si phase shows a complicated morphology and leads to the formation of Si phase with large size. Additionally, the eutectic Si phase with needle-like morphology changes into bar-like or block-like morphology with increasing the pre-annealing temperature. At the same time, it is also clear to observe that clustering of the eutectic Si phase occurred after pre-annealing at 300 to 400 °C. This indicates that the primary Si phase grows by attachment of not only Si atoms but also Si−Si clusters.

Figure 4 shows the XRD patterns of the gas-atomized Al−Si alloy powders before and after annealing. It can be seen that all diffraction peaks are attributed to Al and Si phases, and no additional intermetallic or compound can be observed. Therefore, no detrimental reaction occurred during the fabrication and annealing process. However, the diffraction peaks of Si phase are more visible owing to the precipitation and growth of supersaturated Si atoms.

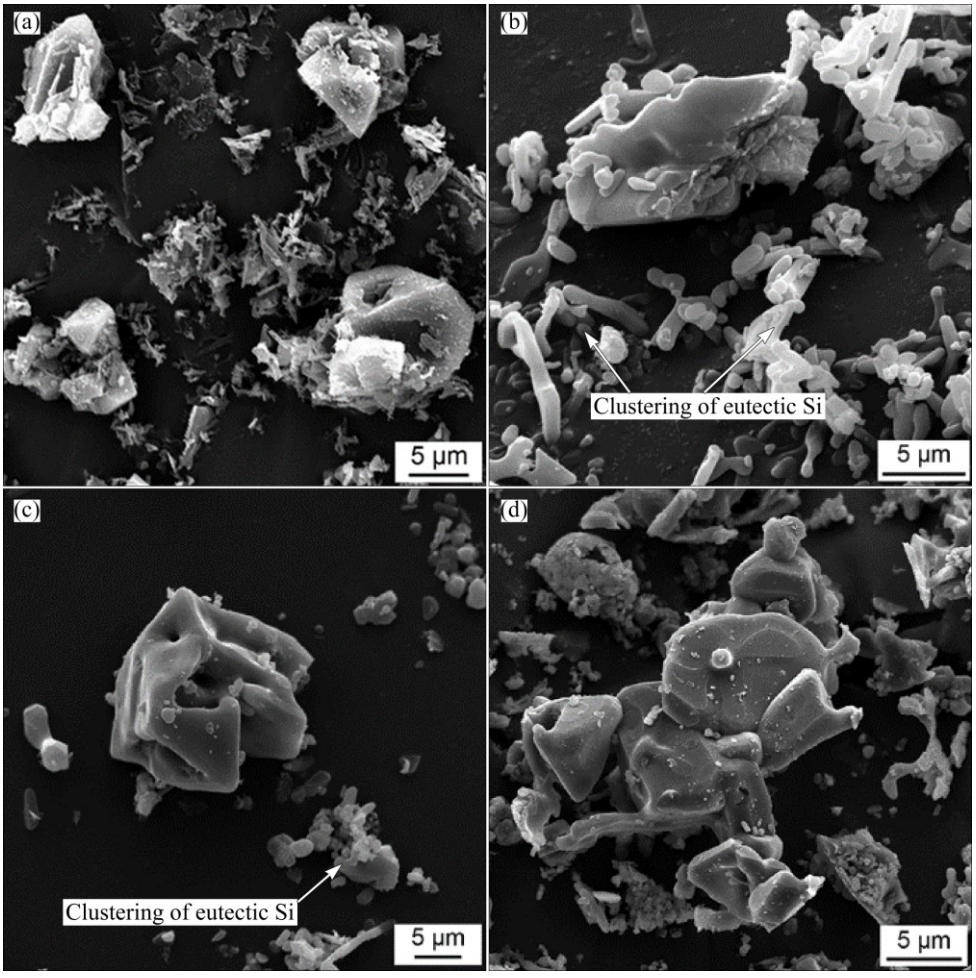

Fig. 3 Morphologies of primary and eutectic Si phases as-atomized (a) and pre-annealed at 300 °C (b), 400 °C (c), and 450 °C (d)

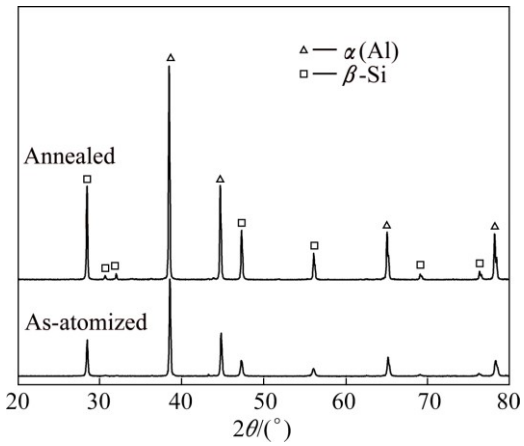

Fig. 4 XRD patterns of gas-atomized Al−Si alloy powders before and after pre-annealing at 400 °C

Figure 5 illustrates the average size of primary Si phase and the microhardness as a function of the pre-annealing temperature. No observable coarsening of the Si phase is found after pre-annealing at temperatures below 250 °C. However, with further increasing the temperature, the size of Si phase increases quickly from 1.78 μm at as-atomized state to 4.56 μm after pre-annealing at 450 °C. Generally, the Si phase grows by attachment of Si atoms to the surface of pre-existed Si particles. The diffusion rate of Si atoms plays an important role in the growth of Si phase. As a thermal-activated process, the diffusion of Si atoms will become easier with increasing temperature, which accelerates the diffusion rate to a great extent. Therefore, the size of Si phase increases evidently with increasing the pre-annealing temperature.

The variation of mechanical property of the powder particles was studied through the Vickers microhardness measurements (Fig. 5). Microhardness of the powder decreases from HV 106 at the as-solidified state to HV 71 after pre-annealing at 450 °C. The supersaturation of Si atoms owing to the high undercooling during atomization and the densely distributed eutectic Si phase in Al matrix result in the high microhardness. A rapid decrease is observed as the pre-annealing temperature increases from 200 to 400 °C. However, nearly identical microhardness values are obtained when the pre-annealing temperature is higher than 400 °C. The main reason is that, in the thermal activation, precipitations of supersaturated atoms weaken the effect of solid solution strengthening on the Al matrix. Additionally, the relaxation of lattice distortion and decrease of dislocation density also contribute to the softening of Al matrix.

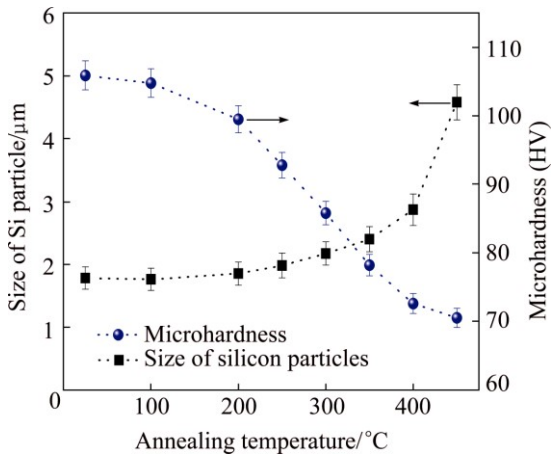

Fig. 5 Size of primary Si phase and microhardness of Al matrix with increasing pre-annealing temperature

3.3 Compaction behavior

Figure 6 shows the compaction and densification rate (increment of relative density) curves of the gas-atomized Al−Si alloy powders annealed at various temperatures. The density related to the zero applied pressure is the tap density of 45.6% (Fig. 6(a)). In general, the compaction curves are similar to those of conventional metallic powders, i.e., the relative density increases with increasing the applied pressure with a decelerating densification rate (Fig. 6(b)). The compactibility is generally indicated by the extent of

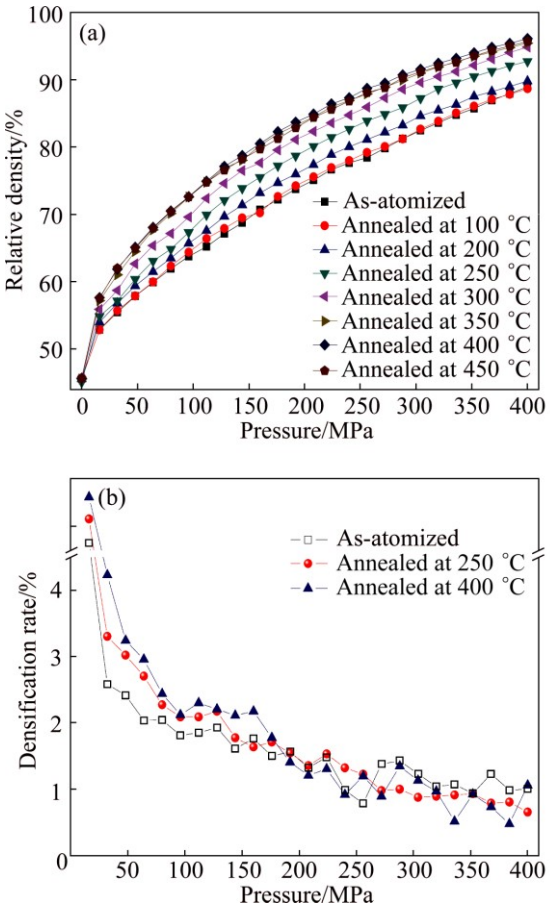

Fig. 6 Compaction (a) and densification rate (b) curves of Al−Si alloy powders as function of pre-annealing temperature

increased green density after applying a specific compaction pressure. Therefore, the compactibility is gradually improved with increasing the pre-annealing temperature to 400 °C, but is limited above that. The relative density of powder pre-annealed at 400 °C reaches a maximum value of 96.1% after compacting at 400 MPa. Additionally, the deviation in compatibility of the pre-annealed powder is more noticeable with increasing the applied pressure to about 175 MPa, and then the deviation is reduced with higher pressure.

According to the variation of microhardness of Al matrix with increasing the pre-annealing temperature, as shown in Fig. 5, the powders pre-annealed at relatively high temperatures obtain high level of deformation capacity. Owing to the mechanical property difference between the Al matrix and the Si phase, the powders deform through deformation of the soft Al matrix and the hard Si particles are non-deformable. At low compaction pressures, the densification progresses through the deformation of particle surfaces contacting with each other. This suggests that the plastic deformation of Al matrix occurs immediately with little powder rearrangement because the powder is tapped before compaction. It is known that warm compaction reduces the yield pressure of metal powder and enhances the compactibility by improving the contribution of plastic deformation of metal matrix [15]. Therefore, the compactibility of gas-atomized Al−Si alloy powders is gradually improved with decreasing the matrix hardness resulted from the increasing pre-annealing temperature.

In order to explain the densification behavior of gas-atomized hypereutectic Al−Si alloy powders, not only the mechanical property was taken into consideration, but also the morphology and size of Si phases were investigated. During compaction, the Al matrix deforms plastically, the pores decrease in size and amount and the yield stress of the Al matrix increases due to the work hardening effect. Considering the deformation resistance, the primary Si with irregular shapes and sharp edges and the needle-like eutectic Si and dense distribution become a detrimental factor on compatibility. It has been indicated that the matrix should be deformed when inclusions have irregular shape and high surface area [6]. Therefore, due to the characteristics of rapidly solidified microstructure, the as-solidified alloy powders have poor compactibility.

With increasing the pre-annealing temperature to 200 °C and 250 °C, the dissolving of the needle-like eutectic Si phase contributes to the densification. However, at such state, the precipitated Si phase with small size and the primary Si phase with still sharp edges have large specific area and thereby experience increased friction during the compaction.

Spheroidisation of the primary Si and growth of the precipitated Si with increasing the pre-annealing temperature to 400 °C further improve the compactibility. Therefore, the compactibility of powder improves with increasing the pre-annealing temperature. However, the complicated Si particles caused by the clustering of Si−Si phase after pre-annealing at 450 °C blocks the densification process. At low applied pressures, the influence of the Si phase morphology and size on the densification is relatively small, because the rearrangement of powder particles is the dominant densification mechanism. As the applied pressure increases, however, this effect is enhanced due to the work hardening of Al matrix. Such effects of morphology and size of Si phase on the compactibility are similar to those of reinforcement characteristics in composite powder [13,26].

Another possible factor which determines the compactibility is the volume fraction of the Si phase, as the matrix should conduct extra plastic deformation with high volume fraction of reinforcement. Thus, the compactibility of the powders pre-annealed at 450 °C is limited due to the complete precipitation and clustering of the Si phase. The compaction mechanism is usually considered in four stages, but it is unlikely that a single compaction equation will fit well in a single stage because several mechanisms may occur concurrently according to the powder characteristics and pressure level [8,27].

Therefore, the hardness of the Al matrix plays an important role at the initial stage of compaction at low pressures. While, the dissolving of the eutectic Si, growth of the precipitated Si, and spheroidisation of the primary Si contribute to the densification of the pre-annealed powder at high pressures. However, the clustering of Si−Si phase may be detrimental to the densification of hypereutectic Al−Si alloy powders. It is somewhat difficult to identify the size distribution of Si particles which could also influence the compactibility of hypereutectic Al−Si alloy powders. Therefore, it is important to choose a proper pre-annealing temperature for improving the compactibility of rapidly solidified powder.

4 Conclusions

1) Dissolving of the needle-like eutectic phase, precipitation and growth of supersaturated Si, and spheroidisation of the primary Si phase are observed in the rapidly solidified hypereutectic Al−Si alloy depending on the pre-annealing temperature. Clustering of the primary Si phase is observed after pre-annealing at 450 °C, which leads to the quick growth of Si phase. Microhardness of the Al matrix decreases apparently after pre-annealing at 250 to 400 °C.

2) The compactibility of gas-atomized Al−Si alloy powders is improved gradually with increasing the pre-annealing temperature to 400 °C due to the decreased deformation resistance, which can attribute to the Al matrix softening and the evolution of the Si phase morphology and size. However, the compactibility is limited when the pre-annealing temperature is above 450 °C owing to the existence of Si−Si clusters and densely distributed Si phase.

3) Densification deviation of the powders pre-annealed at different temperatures shows that plastic deformation of the Al matrix occurs immediately with little particle rearrangement. The high microhardness of the matrix determines the densification behavior at low pressures, while the size, morphology, and volume fraction of reinforcing phase become more dominant at high pressures.

References

[1] YAMAUCHI I, OHNAKA I, KAWAMOTO S, FUKUSAKO T. Production of rapidly solidified Al−Si alloy powder by the rotatin-water-atomization process and its structure [J]. Journal of the Japan Institute of Metals, 1985, 49(1): 72−77.

[2] MAUSUURA K, KUDOH M, KINOSHITA H, TAKAHASHI H. Precipitation of Si particles in a super-rapidly solidified Al−Si hypereutectic alloy [J]. Materials Chemistry and Physics, 2003, 81(2−3): 393−395.

[3] ZHU Xue-wei, WANG Ri-chu, PENG Jian, PENG Chao-qun. Microstructure evolution of spray-formed hypereutectic Al−Si alloys in semisolid reheating process [J]. Transactions of Nonferrous Metals Society of China, 2014, 24(6): 1766−1772.

[4] TOURRET D, REINHART G, GANDIN C A, ILES G N, DAHLBORG U, CALVO-DAHLBORG M, BAO C M. Gas atomization of Al−Ni powders: Solidification modeling and neutron diffraction analysis [J]. Acta Materialia, 2011, 59(17): 6658−6669.

[5] ENNETI R K, LUSIN A, KUMAR S, GERMAN R M, ATRE S V. Effects of lubricant on green strength, compressibility and ejection of parts in die compaction process [J]. Powder Technology, 2013, 233: 22−29.

[6] DELIE F, BOUVAR D. Effect of inclusion morphology on the densification of powder composites [J]. Acta Materialia, 1998, 46(11): 3905−3913.

[7] WU W, JIANG G, WAGONER R H, DAEHN G S. Experimental and numerical investigation of idealized consolidation: Part 1: Static compaction [J]. Acta Materialia, 2000, 48(17): 4323−4330.

[8] DENNY P J. Compaction equations: A comparison of the Heckel and Kawakita equations [J]. Powder Technology, 2002, 127(2): 162−172.

[9] MORENO M F, OLIVER C J R G. Densification of Al powder and Al−Cu matrix composite (reinforced with 15% Saffil short fibres) during axial cold compaction [J]. Powder Technology, 2011, 206(3): 297−305.

[10] LIU X Y, HU L X, WANG E D. Cold compaction behavior of nano-structured Nd−Fe−B alloy powders prepared by different processes [J]. Journal of Alloys and Compounds, 2013, 551: 682−687.

[11] RAMAKRISHNAN K N, NAGARAJAN R, RAMARAO G V, VENKADESAN S. A compaction study on ceramic powders [J]. Materials Letters, 1997, 33(3−4): 191−194.

[12] SKRINJAR O, LARSSON P L. Cold compaction of composite powders with size ratio [J]. Acta Materialia, 2004, 52(7): 1871−1884.

[13] RAZAVI-TOUSI S S, YAZDANI-RAD R, MANAFI S A. Effect of volume fraction and particle size of alumina reinforcement on compaction and densification behavior of Al−Al_2O_3 nanocomposites [J]. Materials Science and Engineering A, 2011, 528(3): 1105−1110.

[14] HAFIZPOUR H R, SANJARI M, SIMCHI A. Analysis of the effect of reinforcement particles on the compressibility of Al−SiC composite powders using a neural network model [J]. Materials & Design, 2009, 30(5): 1518−1523.

[15] HAFIZPOUR H R, SIMCHI A, PARVIZI S. Analysis of the compaction behavior of Al−SiC nanocomposites using linear and non-linear compaction equations [J]. Advanced Powder Technology, 2010, 21(3): 273−278.

[16] MOAZAMI-GOUDARZI M, AKHLAGHI F. Effect of nanosized SiC particles addition to CP Al and Al−Mg powders on their compaction behavior [J]. Powder Technology, 2013, 245: 126−133.

[17] ABDOLI H, SALAHI E, FARNOUSHI H, POURAZRANG K. Evolutions during synthesis of Al−AlN-nanostructured composite powder by mechanical alloying [J]. Journal of Alloys and Compounds, 2008, 461(1−2): 166−172.

[18] FOGAGNOLO J B, RUIZ-NAVAS E M, ROBERT M H, TORRALBA J M. The effects of mechanical alloying on the compressibility of aluminium matrix composite powder [J]. Materials Science and Engineering A, 2003, 355(1−2): 50−55.

[19] RAZAVI H Z, HALFIZPOUR H R, SIMCHI A. An investigation on the compressibility of aluminum/nano-alumina composite powder prepared by blending and mechanical milling [J]. Materials Science and Engineering A, 2007, 454−455: 89−98.

[20] WARD P J, ATKINSON H V, ANDERSON P R G, ELIAS L G, FARCIA B, KAHLEN L, RODRIGUEZ-IBABE J M. Semi-solid processing of novel MMCs based on hypereutectic aluminium−silicon alloys [J]. Acta Materialia, 1996, 44(5): 1717−1727.

[21] LI Yan-xia, LIU Jun-you, WANG Wen-shao, LIU Guo-qun. Microstructures and properties of Al−45%Si alloy prepared by liquid–solid separation process and spray deposition [J]. Transactions of Nonferrous Metals Society of China, 2013, 23(4): 970−976.

[22] WANGER C. Theory of precipitate change by redissolution [J]. Z Electrochem, 1961, 65(7−8): 581−591.

[23] LIFSHITZ I M, SLYOZOV V V. The kinetics of precipitation from supersaturated solid solutions [J]. Journal of Physics and Chemistry of Solids, 1961, 19(1−2): 35−50.

[24] BIROL Y. Microstructural evolution during annealing of a rapidly solidified Al−12Si alloy [J]. Journal of Alloys and Compounds, 2007, 439(1−2): 81−86.

[25] BAIK K H, SEOK H K, KIM H S, GRANT P S. Non-equilibrium microstructure and thermal stability of plasma-sprayed Al−Si coatings [J]. Journal of Materials Research, 2005, 20(8): 2038−2045.

[26] ASGHARZADEH H, SIMCHI A, KIM H S. A plastic-yield compaction model for nanostructured Al6063 alloy and Al6063/Al_2O_3 nanocomposite powder [J]. Powder Technology, 2011, 211(2−3): 215−220.

[27] TAVAKOLI A H, SIMCHI A, SEYED R S M. Study of the compaction behavior of composite powders under monotonic and cyclic loading [J]. Composites Science and Technology, 2005, 65(14): 2094−2104.

预退火对气雾化 Al−Si 合金粉末显微组织和压制性能的影响

蔡志勇[1,2]，张 纯[1,2]，王日初[2]，彭超群[2]，邱 科[2]，王乃光[2]

1. 江西理工大学 材料科学与工程学院，赣州 341000；
2. 中南大学 材料科学与工程学院，长沙 410083

摘 要：研究预退火温度对气雾化 Al−27%Si 合金粉末压制性能的影响，并分析退火粉末的显微组织和硬度。预退火不仅降低 Al 基体硬度，而且导致针状共晶 Si 相熔解、过饱和固溶 Si 原子析出和长大以及初晶 Si 相球化。合金粉末的压制性能随着退火温度升高至 400 °C 而逐渐提高；但是，由于出现 Si−Si 相缠结和密集分布的 Si 颗粒，粉末的压制性能在退火温度高于 400 °C 时反而有所下降。粉末在 400 °C 退火 4 h 后，其相对密度最大达到 96.1%。另外，预退火合金粉末压制性能的差异在压制压力为 175 MPa 时达到最大。因此，通过合适的预退火处理可以大幅提高气雾化 Al−Si 合金粉末的室温压制性能。

关键词：Al−Si 合金；压制性能；快速凝固；退火；显微组织

(Edited by Xiang-qun LI)